Journal of Physics: Conference Series **1342** (2020) 012071 doi:10.1088/1742-6596/1342/1/012071

Energy response and position reconstruction in the DEAP-3600 dark matter experiment

Stefanie Langrock on behalf of the DEAP-3600 collaboration
SNOLAB, 1039 Regional Road 24, Creighton Mine #9, Lively, ON, Canada, P3Y 1N2
E-mail: stefanie.langrock@snolab.ca

Abstract. DEAP-3600 is a dark matter WIMP (Weakly Interacting Massive Particles) search experiment, which aims to detect nuclear recoils from WIMP scattering in a liquid argon target. At WIMP masses of 100 GeV, DEAP-3600 has a projected sensitivity of 10^{-46} cm^2 for the spin-independent elastic scattering cross section of WIMPs. The beta emissions from the intrinsic ^{39}Ar present in the natural Ar target, as well as external calibration sources, can be used to tune the energy calibration and position reconstruction in the energy region of interest (ROI) for WIMP signals. These proceedings will present the techniques used to determine the energy response and position reconstruction in DEAP-3600. Using these techniques, the light yield was found to be LY $= 7.36^{+0.61}_{-0.52}$(fit syst.) $\pm$ 0.22(SPE syst.) PE/keV$_{ee}$ with a fiducial mass for WIMP detection of 2 223 $\pm$ 74 kg for the first data set.

1. Introduction

The Dark Matter Experiment using Argon Pulse-shape discrimination (DEAP) is designed for direct WIMP dark matter detection. Located 2 km underground at the SNOLAB facility in Lively, Ontario, Canada, DEAP-3600 was filled with a 3 322 $\pm$ 110 kg single-phase liquid argon (LAr) target for the analysis presented here, with the potential to increase the target mass to 3 600 kg. The target mass is contained in an acrylic vessel (AV) with a 850 cm radius surrounded by 255 Hamamatsu R5912-HQE photomultiplier tubes (PMTs). The PMTs are connected to the AV via 45 cm long acrylic light guides (LGs) for neutron shielding and to contain the light of events. The structure is enclosed in a stainless steel shell immersed in an 8 m diameter shield tank filled with ultra-pure water. Attached to the steel shell are 48 muon veto PMTs [1].

Passing particles are detected via the emission of scintillation light from the LAr target. Unstable argon dimers are produced from particle recoils on the argon atoms. The two possible excited dimer states have a distinct lifetime of 6 ns or $\sim$ 1300 ns, the production ratio of which depends on the linear energy transfer from the incoming particle. Electromagnetic events mostly create long-lived triplet states, whilst nuclear recoils predominantly populate the short-lived triplet state. The ratio of prompt light over all the light in the event can therefore be used to distinguish nuclear recoils from β-decays and γ interactions. This analysis method is referred to as pulse-shape discrimination (PSD) [2]. The energy of the recoil particles is determined by a charge integration of the PMTs. The detected charge can be converted to the number of observed photoelectrons (PE) using a charge division method based on the PMT calibration [3].

2. Considered calibration sources

Several calibration sources are used in DEAP-3600 for position and energy calibration of the detector. They can be divided into optical and radioactive sources as well as internal and external sources. This document focuses on two radioactive sources: ^{39}Ar (internal) and ^{22}Na (external). Both sources are briefly described in this section.

^{39}Ar is a β^--emitter with an endpoint energy of $Q = 565\,\text{keV}$. It is produced from cosmic ray interactions on ^{40}Ar and is therefore present in the natural LAr used in DEAP-3600 with an activity of approximately 1 Bq/kg. It is isotropically distributed within the LAr, providing a good calibration source to test the uniformity of the energy response of the target material. It can also be used to develop position fitter debiasing algorithms and provide a measurement of the fiducial mass. ^{39}Ar is the dominant electromagnetic background at low energies close to the WIMP ROI.

^{22}Na is an external radioactive calibration source, which is deployed during source runs in one of the DEAP-3600 calibration tubes located around the steel shell (see Figure 1). It decays to an excited state of ^{22}Ne via a β^+-decay, which de-excites by emitting a 1275 keV γ. The positron from the ^{22}Na decay annihilates in the surrounding material, resulting in the emission of two back-to-back 511 keV γ. This topology provides an excellent tagging scheme for ^{22}Na decays to distinguish them from backgrounds.

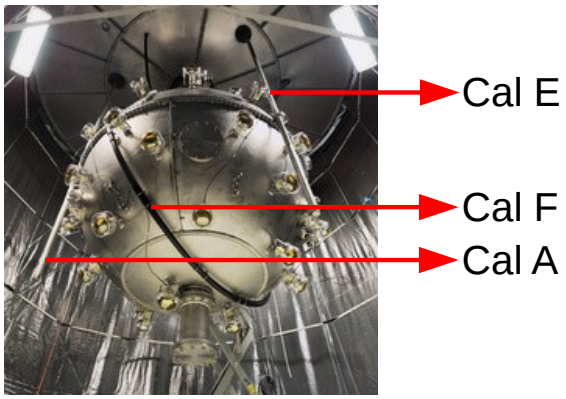

Figure 1. The DEAP-3600 calibration tubes located outside of the steel shell. ^{22}Na deployments are carried out through CAL F.

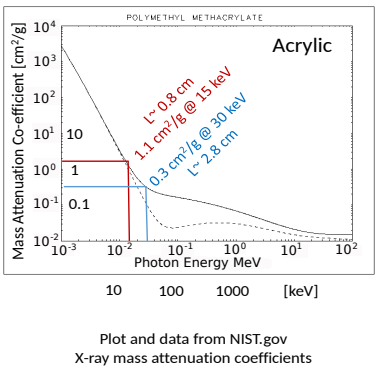

Figure 2. The mass attenuation co-efficient of photons in acrylic at different energies from the NIST database. For two photon energies, the mean path of the photons is indicated.

The mono-energetic γ's from the ^{22}Na decay provide good calibration lines, however we observe another energy feature in the ^{22}Na energy spectrum at low energies. This feature is a result of high energy gammas scattering and loosing energy in the material between source and LAr target. It is a combination of different event topologies which most likely result in a gamma energy of 30/40 keV entering the LAr. Its shape and position is reproduced by the MC (see Figure 3). Figure 2 shows the mass attenuation coefficient of photons at different energies in acrylic, one of the materials the photons pass on their way to the target volume. Photons with energies below 30/40 keV have a very short mean path before being absorbed in the material by the photoelectric effect. The emitted electrons are not observed in the target volume, leading to a rising edge in the ^{22}Na energy spectrum at low energies (see Figure 3). This feature is a useful tool to determine the fiducial leackage of surface events with energies close to the expected WIMP energies and to achieve a good understanding of the detector energy response at low energies at several positions around the detector.

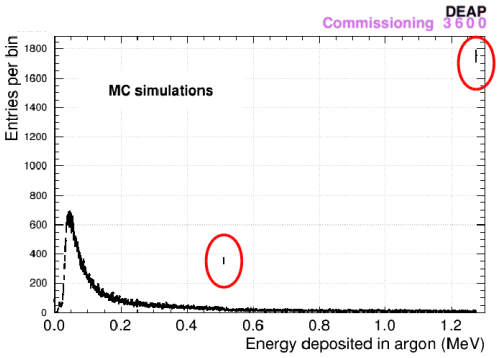

Figure 3. The true energy deposited in the LAr scintillator from a ^{22}Na simulation.

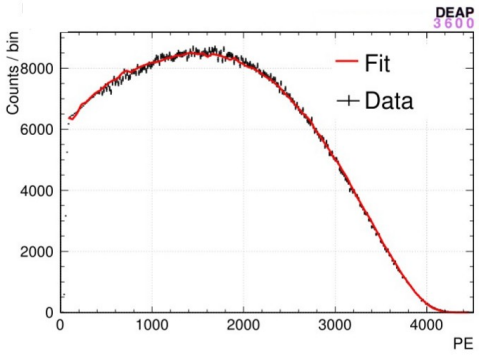

Figure 4. Fit to the ^{39}Ar spectrum as detected by DEAP-3600. The fit function (red) was constructed from ^{39}Ar MC.

3. Energy calibration

The energy response in the detector is defined by the light yield (LY) which translates the measured PE spectrum into energy in keV$_{ee}$. The light yield was determined by fitting the measured ^{39}Ar and ^{22}Na spectra to PE spectra or spectra based on the true energy (Edep) in keV extracted from Monte Carlo (MC) simulations. In both cases, the PE and Edep MC spectra were scaled in two dimensions, x (energy) and y (number of observed events) to match the data. For the scaling in energy a quadratic energy response function with offset of the form $T_{\text{eff}}\,(\text{PE}) = c_0 + c_1 \cdot \text{PE} + c_2 \cdot 10^{-6} \cdot \text{PE}^2$ was used, leading to three energy scale fit parameters in x. This form of energy response was chosen to account for uncertainties from PMT saturation effects and effects from PMT afterpulsing (compare also [3]) and uncertainties from the radial position of the decays.

The fit to the ^{39}Ar spectrum is shown in Figure 4. The fit function was defined from a ^{39}Ar MC PE spectrum assuming the energy response function as described above. The same approach was used on fitting the ^{22}Na spectrum assuming the same quadratic-with-offset energy response of the detector. However, two different approaches were applied to fit the entire ^{22}Na spectrum and to only fit the low energy feature up to 1000 PE. The low energy fit (Figure 5) was performed using a ^{22}Na MC PE spectrum, similar to the fit on ^{39}Ar. The fit on the full ^{22}Na spectrum was carried out with the Edep spectra of 511 keV and 1275 keV γs simulated separately at the source position (Figure 6). For this fit the region between the 511 keV and the 1275 keV peak was excluded since the method did not allow for coincidence events from these spectra. Both ^{22}Na fit functions included a ^{39}Ar contribution extracted from a data run close in time to the ^{22}Na deployment.

4. Position reconstruction

The position reconstruction in DEAP-3600 is based on the charge patterns of the PMTs. All WIMP-like interactions are point-like sources, thus PMTs closer to the source are expected to be hit by more photons and therefore detect higher charges. In this approach the vertex resolution improves towards the edge of the detector. The resulting charge pattern is detector dependent and consequently requires training of the position-finding algorithms.

A high statistics MC of an isotropically distributed source with a full detector model including all the optics was produced to train the fitters. Using this sample, a look-up table was created using the true detector position and the charge pattern observed by the PMTs. When the detector data is processed, the PMT charge pattern of each event is read-out and compared to

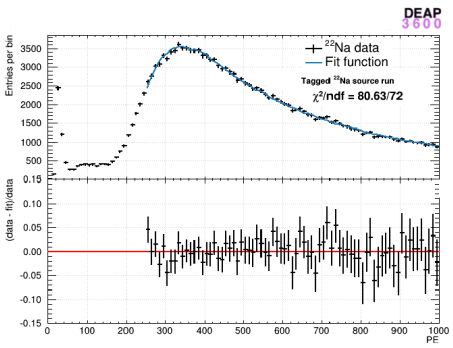

Figure 5. A fit to the low energy spectrum of ^{22}Na data taken in DEAP-3600. The fit function was defined from ^{22}Na MC. The fit was restricted to $250 - 1000$ PE. The lower fit boundary was chosen to avoid uncertainties from trigger efficiencies.

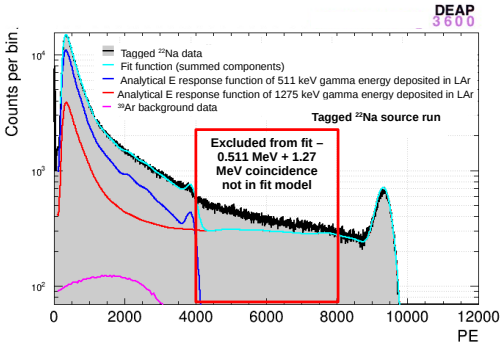

Figure 6. A fit to the full energy spectrum of ^{22}Na data taken in DEAP-3600. The main fit components are 511 keV γ and 1275 keV γ simulations. The region between $4000 - 8000$ PE was excluded from the fit.

the look-up table using a minimisation algorithm. The fitter returns the best match as the fitted event position.

Radial biases introduced to the position reconstruction, e.g. by uncertainties in the optical model of the detector, can be corrected using ^{39}Ar events which are uniformly distributed in the detector. Similarly to the initial fitter training, a high statistics ^{39}Ar MC with full detector simulation was used. A map for different event energies was generated, which contains correction factors based on the MC truth position versus the reconstructed positions of the MC events. These correction factors can then be applied to the fitted event position. An example of debiased ^{39}Ar data is shown in Figure 7. This debiasing algorithm trained from ^{39}Ar can also be applied to ^{22}Na data, as shown in Figure 8.

5. Results

The techniques presented here were used to determine the energy response and fiducial volume for the first 4.44 d data set, which is presented in [4]. To evaluate the light yield, the low energy fit to the ^{22}Na spectrum and the ^{39}Ar fit were combined in a weighted average to determine the global energy response function T_{eff} [keV$_{ee}$] shown in Figure 9. The averaged energy scale fit paramaters are $c_0 = 1.15 \pm 0.50\,\text{keV}_{ee}$, $c_1 = 0.121 \pm 0.004\,\text{keV}_{ee}\text{PE}^{-1}$ and $c_2 = (1.32 \pm 0.08) \times 10^{-6}\,\text{keV}_{ee}\text{PE}^{-2}$. The uncertainties on the fit parameters were scaled for both fits by $\sqrt{\chi^2_{ndf}}$ before the weighted average was evaluated to account for systematic uncertainties. Both fits agree within their uncertainties. The full spectrum ^{22}Na fit was not included due to the unaccounted area between the two γ lines. The measured light yield in the detector at 80 PE is

$$\text{LY} = 7.36^{+0.61}_{-0.52}(\text{fit syst.}) \pm 0.22(\text{SPE syst.})\,\text{PE/keV}_{ee} \quad (1)$$

Since ^{22}Na is an external source, the debiased event positions of the low energy ^{22}Na helped determine fiducial cut parameters at energies close to the WIMP ROI based on the leakage of ^{22}Na events. After applying these cuts, the ^{39}Ar rates were used to determine the fiducial mass of the detector, which was found to be consistent with $2\,223 \pm 74$ kg of LAr.

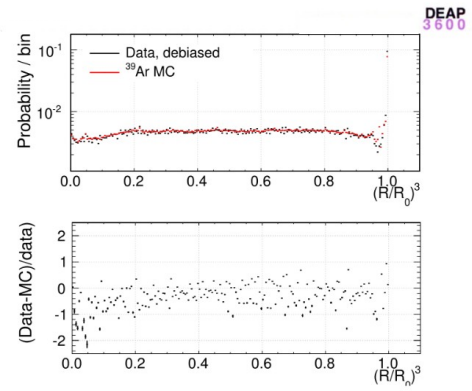

Figure 7. The reconstructed radii of ^{39}Ar data events after applying the debiasing to the position reconstruction, compared to ^{39}Ar MC. The residual between data and MC is presented in the bottom plot.

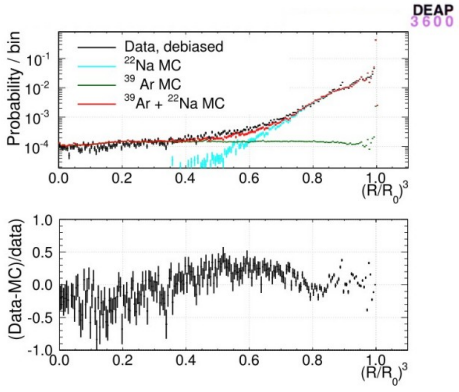

Figure 8. The reconstructed radii of ^{22}Na data events after applying the debiasing to the position reconstruction. ^{22}Na and ^{39}Ar MC as well as their sum are also displayed. The bottom plot shows the residual between the ^{22}Na data and the summed MC.

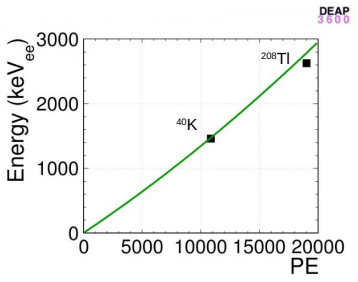

Figure 9. Energy response function of the DEAP-3600 experiment calculated using the weighted average of the fit results from the ^{39}Ar fit and the low energy ^{22}Na fit presented in Figures 4 and 5. The two points at PE $>$ 10000 are the γ lines from ^{40}K and ^{208}Tl are added as a cross check to compare to the extrapolated function.

6. Ackowledgements

This work is supported by the Natural Sciences and Engineering Research Council of Canada, the Canadian Foundation for Innovation (CFI), the Ontario Ministry of Research and Innovation (MRI), and Alberta Advanced Education and Technology (ASRIP), Queens University, University of Alberta, Carleton University, DGAPA-UNAM (PAPIIT No. IA100316), European Research Council (ERC StG 279980), the UK Science & Technology Facilities Council (STFC) (ST/K002570/1), the Leverhulme Trust (ECF-20130496). Studentship support by the Rutherford Appleton Laboratory Particle Physics Division, STFC and SEPNet PhD is acknowledged. We thank SNOLAB and its staff for support through underground space, logistical and technical services. SNOLAB operations are supported by CFI and the Province of Ontario MRI, with underground access provided by Vale at the Creighton mine site. We thank Compute Canada, Calcul Québec and the Center for Advanced Computing at Queens University for providing the excellent computing resources required to undertake this work.

7. References

[1] Kuźniak M. et al. 2016 *Nuclear and Particle Physics Proceedings* **273–275** 340–346
[2] Amaudruz P.-A. et al. 2016 *Astroparticle Physics* **85** 1–23
[3] The DEAP Collaboration 2017 *arXiv:1705.10183*
[4] Amaudruz P.-A. et al. 2017 *arXiv:1707:08042*